J Biomol NMR (2010) 48:113–121
DOI 10.1007/s10858-010-9443-7

ARTICLE

Optimizing ^{19}F NMR protein spectroscopy by fractional biosynthetic labeling

Julianne L. Kitevski-LeBlanc · Ferenc Evanics · R. Scott Prosser

Received: 19 July 2010 / Accepted: 27 July 2010 / Published online: 24 August 2010
© Springer Science+Business Media B.V. 2010

Abstract In protein NMR experiments which employ nonnative labeling, incomplete enrichment is often associated with inhomogeneous line broadening due to the presence of multiple labeled species. We investigate the merits of fractional enrichment strategies using a monofluorinated phenylalanine species, where resolution is dramatically improved over that achieved by complete enrichment. In NMR studies of calmodulin, a 148 residue calcium binding protein, ^{19}F and ^{1}H-^{15}N HSQC spectra reveal a significant extent of line broadening and the appearance of minor conformers in the presence of complete (>95%) 3-fluorophenylalanine labeling. The effects of varying levels of enrichment of 3-fluorophenylalanine (i.e. between 3 and >95%) were further studied by ^{19}F and ^{1}H-^{15}N HSQC spectra, ^{15}N T_1 and T_2 relaxation measurements, ^{19}F T_2 relaxation, translational diffusion and heat denaturation experiments via circular dichroism. Our results show that while several properties, including translational diffusion and thermal stability show little variation between non-fluorinated and >95% ^{19}F labeled samples, ^{19}F and ^{1}H-^{15}N HSQC spectra show significant improvements in line widths and resolution at or below 76% enrichment. Moreover, high levels of fluorination (>80%) appear to increase protein disorder as evidenced by backbone ^{15}N dynamics. In this study, reasonable signal to noise can be achieved between 60–76% ^{19}F enrichment, without any detectable perturbations from labeling.

Keywords ^{19}F NMR · Calmodulin · Fractional labeling · Biosynthetic labeling · 3-fluorophenylalanine

Abbreviations

3-FPhe	3-fluorophenylalanine
CaM	Calmodulin
NMR	Nuclear magnetic resonance

Introduction

Fluorinated amino acids and amino acid analogues are ubiquitously used to understand or manipulate the physical properties of proteins (Akcay and Kumar 2009; Danielson and Falke 1996; Geddes 2009). In the latter case, it is the change in the physical and chemical properties of the protein that are of interest. For example, fluorinated leucine and valine are known to act as strong helix stabilizers (Bilgiçer et al. 2001) while both fluorinated aromatics and aliphatics have been shown to stabilize the protein fold and provide protection from heat-denaturation and proteolysis (Tang et al. 2001; Woll et al. 2006). This stabilization is attributed to the increased hydrophobicity of fluorocarbons relative to hydrocarbons, and the preference for fluorine-fluorine interactions, which are stronger than the classic hydrophobic effect. In the majority of spectroscopic applications, the goal is to observe the protein in its most unadulterated form—that is, free from probe-induced structural, functional or dynamic perturbations.

NMR and fluorescence studies of proteins often make use of fluorinated amino acids which are generally assumed

Electronic supplementary material The online version of this article (doi:10.1007/s10858-010-9443-7) contains supplementary material, which is available to authorized users.

J. L. Kitevski-LeBlanc · F. Evanics · R. Scott Prosser (✉)
Department of Chemistry, University of Toronto, UTM,
3359 Mississauga Rd., North Mississauga, ON L5L 1C6, Canada
e-mail: scott.prosser@utoronto.ca

R. Scott Prosser
Department of Biochemistry, University of Toronto,
Toronto, ON M5S 1A8, Canada

to be isosteric with their native counterparts. Such studies may investigate binding (Anderluh et al. 2005; Broos et al. 2004; Luck and Falke 1991), catalysis (Quint et al. 2006; Rozovsky et al. 2001) and folding or unfolding (Bann et al. 2002; Li and Frieden 2007; Schuler et al. 2002; Visser et al. 2009). Indeed, in the majority of applications the usual mantra is that because the fluorine atom is less than 20% larger than that of hydrogen there is little perturbation to be concerned with, particularly when the substitution involves mono-fluorinated amino acids. However, to strictly be able to claim that there are no perturbations resulting from such incorporation, a stringent series of functional and structural investigations should be performed as a function of enrichment of the fluorinated amino acid(s). Several authors have observed probe-induced perturbations arising from fluorinated aromatics to varying degrees (Duewel et al. 2001; Luck and Falke 1991; Xiao et al. 1998), though a systematic study of enrichment has to our knowledge not been conducted. Although the van der Waals radius of the fluorine atom is comparable to that of hydrogen, the packing density of the protein hydrophobic core may exceed 75% (Woolfson 2001), leaving little room for modified aromatics. While there are many examples where fluorinated residues do not perturb protein structure (Campos-Olivas et al. 2002), some caution is warranted, particularly in studies of intermediates or in situations where the fluorine probes are concentrated in the protein interior.

In ^{19}F NMR studies of proteins, full enrichment is desired to avoid multiple conformers and the predominance of inhomogeneous line broadening. We show in this study that exactly the opposite is the case; namely, lower enrichment leads to substantially better spectra, with fewer minor conformers and narrower line widths. Specifically, we examine structural and dynamic perturbations arising from biosynthetic labeling of calmodulin (CaM) with 3-fluorophenylalanine (3-FPhe). We then explore the utility of fractional labeling through the combined enrichment of phenylalanine and 3-fluorophenylalanine, and the consequences to NMR spectra as well as thermal stability of CaM. Ideal labeling levels were achieved at or below 76% random enrichment of 3-FPhe, where perturbations were found to be minimal while NMR experimental time was not significantly hampered.

Results and discussion

Full and fractional labeling of calmodulin: effects on ^{19}F NMR spectra

Calmodulin is a ubiquitous calcium sensor protein which binds and activates a variety of enzymes in response to an increase in intracellular calcium levels (Hoeflich and Ikura 2002). CaM is a 148 residue, acidic protein organized into two structurally similar calcium binding domains connected by a flexible linker. Four calcium ions are coordinated by a pair of canonical EF-hand motifs in each of the N-terminal (residues 1–73) and C-terminal (83–148) domains with pentagonal bipyramidal symmetry. Upon calcium coordination a well-characterized conformational transition occurs exposing hydrophobic patches in each domain for protein binding (Crivici and Ikura 1995). There are eight phenylalanine residues in *Xenopus laevis* CaM, whose positions are indicated in the ribbon diagram representation of the X-ray structure in Fig. 1a. These residues (i.e. F12, F16, F19, F65, and F68 in the N-terminal domain and F89, F92, and F141 in the C-terminal domain) are highly conserved among species. Phenylalanine residues contribute to the stabilization of the hydrophobic core and have been implicated in peptide binding and activation (Okano et al. 1998). CaM samples enriched with 3-FPhe at 3, 6, 60, 76, >80 and >95%, were prepared as described in the Materials and Methods section, and the resulting ^{19}F NMR spectra are shown in Fig. 1b. Resonance assignments shown were determined in an earlier study (Kitevski-Leblanc et al. 2010).

The enrichment levels, which were obtained using a protocol described in the Materials and Methods section, do not correlate well with the ratios of 3-FPhe to Phe added, in the series of proteins examined. Although it is known that an aminoacyl-tRNA synthetase will exhibit a preference for the corresponding native amino acid, and that this preference varies among, at least the aromatic amino acids (Luck and Falke 1991), one would expect a trend in the fraction of a fluorinated analogue added and the incorporation level obtained. Higher concentrations of 3-FPhe might cause significant stalling of protein translation, assuming tRNA synthetase off rates of 3-FPhe and Phe are different, unforeseen toxicity issues, solubility issues, or any number of variables. If fractional labeling were to be attempted in another system, a range of fluorinated amino acid to natural amino acid ratios would need to be tested.

As shown in Fig. 1b, it is evident from the ^{19}F NMR spectra that labeling levels greater than 80% result in significant overlap of resonances, particularly of F12, F16 and F89, and a great range of peak line widths as well as the presence of additional minor conformers. The possibility that the minor peaks observed correspond to unequal populations of two conformations associated with 180° rotation about the Cβ-Cγ bond of the 3-FPhe residues can be addressed by comparison to fluorine spectra obtained using a symmetric probe, such as 4-fluorophenylalanine, which, from the perspective of the fluorine nucleus, would not be expected to distinguish between these two conformations of the aromatic ring. Indeed ^{19}F 1D and ^{1}H-^{15}N

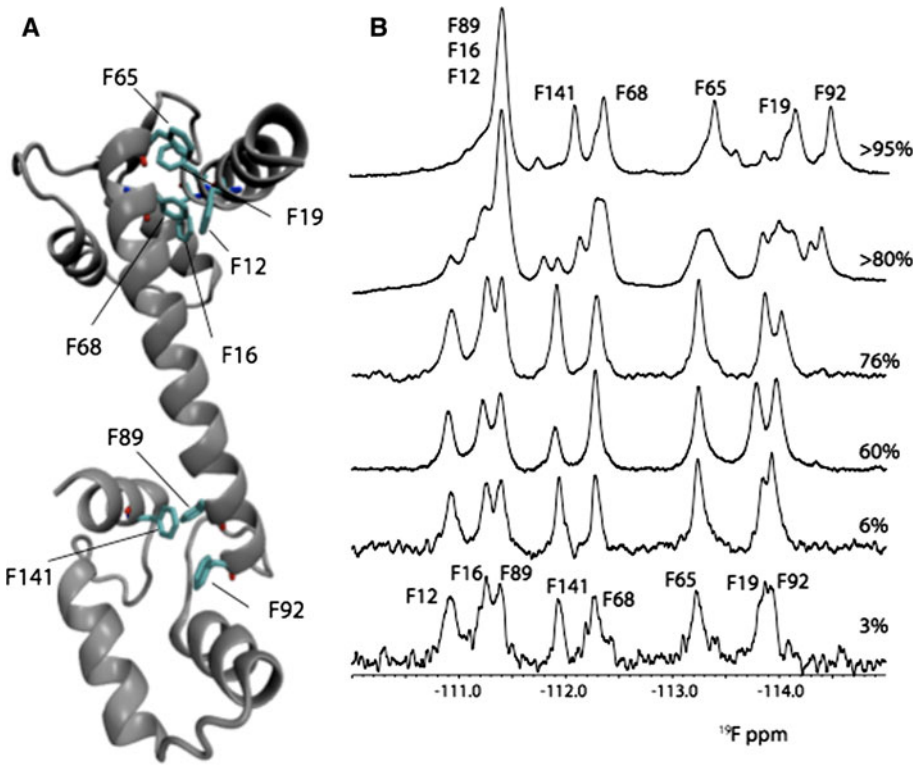

Fig. 1 **a** X-ray structure of calmodulin (PDB file 1CLL) showing the location of the eight phenylalanine residues. **b** ^{19}F NMR spectra of calmodulin enriched with 3 to >95% 3-FPhe. Peak assignments were obtained previously (Kitevski-Leblanc et al. 2010)

HSQC spectra (Supplementary Figure S1 and S2) of CaM labeled with >95% 4-fluorophenylalanine reveal a range of peak line widths, additional minor conformers and chemical shift perturbations, as observed with high levels of 3-FPhe labeling. Note that there does not appear to be any single problematic residue from the perspective of enrichment. Rather, both domains of CaM exhibit broadening and multiple conformers and these cumulative perturbations associated with enrichment of 3-fluorophenylalanine are significantly attenuated at or below 76% enrichment. From the perspective of spectral quality and experimental time, a convenient enrichment level is on the order of 66%.

An obvious concern with partial labeling strategies is the presence of multiple conformers, each corresponding to a specific pattern of label incorporation. For ^{19}F NMR in particular, the presence of multiple conformations may result in additional peaks producing complicated spectra, or an increase in line widths due to inhomogeneous broadening. Spectral line widths are characterized by homogeneous and inhomogeneous contributions arising from both dynamics, slow exchange between spectroscopically distinct states, and to some extent, field inhomogeneities. To characterize the inhomogeneous contribution to the observed ^{19}F line widths at various levels of ^{19}F incorporation we compared ^{19}F line widths to ^{19}F transverse relaxation ($1/T_2$) rates. Contributions from inhomogeneity in the magnetic field were kept nearly constant between protein samples by comparing the line width of an internal standard where we assumed this contribution to be equal among samples when the standard peak line width was within 1 Hz between samples. The $1/T_2$ and line width data for each residue in the 76 and >95% labeled samples are shown in Table 1. The data suggest that ^{19}F line widths are on average reduced by almost 50% under conditions of fractional labeling. This is a significant point, as a reduction in peak widths by half translates to a potential $\sqrt{2}$ increase in sensitivity and enhanced spectral resolution.

The origin of inhomogeneous line broadening is of concern, particularly in situations where fractional labeling strategies are employed. Assuming that inhomogeneous line broadening arises primarily from the co-existence of CaM species with randomly distributed fractional fluorine enrichment, one would expect the greatest line widths to be observed at ~50% fluorine labeling efficiency where there are 2^8 equally probable species in solution. However, as shown in Fig. 1, ^{19}F line widths at 60% fluorine labeling are very similar to those in all fractionally labeled samples below 80%. Moreover, inhomogeneous broadening, which might be expected to result from a multitude of ^{19}F-labeled states, is actually smaller at 76% than that seen at >95% enrichment (i.e. $\Delta 1/T_2^*$ is on average 76.4 vs. 170.3 Hz for 76 and >95% enrichment, respectively). Line widths are independent of labeling efficiency between 3 and 76% enrichment, suggesting that the existence of fractional enrichment levels has little or no effect on line broadening. Rather, the marked increase in both homogeneous and

Table 1 ^{19}F transverse relaxation data ($1/T_2$), line widths ($1/T_2^*$) and the difference $\left[\Delta(1/T_2) = 1/T_2^* - 1/T_2\right]$ for >95 and 76% fluorine labeled calmodulin

Residue	$1/T_2$ (s^{-1})	$1/T_2^*$ (s^{-1})	$\Delta(1/T_2)$
	>95%		
12/16/89	90.3 ± 3.6	303.1 ± 2.0	217.3 ± 0.1
141	64.0 ± 2.6	182.8 ± 2.0	96.82 ± 0.1
68	60.2 ± 1.9	156.4 ± 2.0	96.1 ± 0.1
65	67.9 ± 1.9	293.9 ± 2.0	225.96 ± 0.1
19	69.1 ± 5.31	302.7 ± 2.0	213.63 ± 0.1
92	60.5 ± 6.1	136.7 ± 2.0	76.2 ± 0.1
	76%		
12	63.1 ± 7.0	162.7 ± 2.0	79.57 ± 0.1
16	71.3 ± 3.5	211.7 ± 2.0	140.43 ± 0.1
69	59.3 ± 6.3	103.3 ± 2.0	44.01 ± 0.1
141	60.6 ± 2.8	86.8 ± 2.0	26.2 ± 0.1
66	44.0 ± 3.0	136.8 ± 2.0	92.33 ± 0.1
66	44.0 ± 3.4	143.8 ± 2.0	99.31 ± 0.1
19	60.5 ± 4.2	87.3 ± 2.0	26.73 ± 0.1
92	54.6 ± 5.8	156.1 ± 2.0	101.51 ± 0.1

inhomogeneous broadening observed above 80% enrichment is likely a result of intermediate and slow conformational dynamics resulting from packing perturbations.

Effects on ^{1}H-^{15}N HSQC spectra and ^{15}N dynamics

^{1}H-^{15}N HSQC spectra of non-fluorinated and fluorinated versions of the protein are often compared as a qualitative measure of structural perturbations originating from the fluorinated amino acid probe. In general, spectral discrepancies between non-labeled and labeled proteins are minor and when assignments are available, they are largely associated with residues in the vicinity of the fluorine probe. An overlay of ^{1}H-^{15}N HSQC spectra of 60% and >95% 3-FPhe enriched CaM, each with an analogous spectrum of the non-fluorinated protein are shown in Fig. 2. It is immediately clear that the >95% 3-FPhe enriched protein exhibits increased line widths, as well as significant chemical shift perturbations, most of which are absent in the 60% 3-FPhe enriched sample. The normalized chemical shift perturbations for 6, 60 and >95% ^{19}F labeled 3-FPhe CaM are plotted as a function of residue in Fig. 3a; and reveal moderate perturbations at low levels of incorporation and dramatic perturbations at >95% ^{19}F labeling. In addition to the overall reduced spectral quality, there are two distinct populations of several, well-resolved, N-terminal residues (25, 28, 31, 33, 35, 37, 61, and 63) at higher enrichment levels. An example is shown in the inset of Fig. 2, which focuses on Gly-33. Spectra associated with ^{19}F labeling levels above 6% all exhibit an equilibrium between these two N-terminal conformations, which represent a native and nonnative state as evidenced by the chemical shifts. The free energy associated with this equilibrium at 37°C has been calculated for the relevant labeling efficiencies and the results are collected in Table 2. The data indicate that the nonnative N-terminal conformation is favored only under conditions of full (>95%) labeling, while levels of 60 or 76% ^{19}F labeling provide reasonably uniform samples with stabilities of approximately 4 kT.

Spin–lattice (R_1) and spin–spin (R_2) relaxation rates of backbone amide nitrogen atoms were measured for the 6, 60 and >95% ^{19}F labeled CaM samples. The results are plotted as the difference in a given rate from the non-fluorinated protein for each assignable residue in Fig. 3b, c. As expected, the general trend shows larger deviations from the non-fluorinated protein for higher levels of ^{19}F labeling for both R_1 and R_2. R_1 generally increases with greater 3-FPhe enrichment, while R_2 values decrease. Larger R_1 values and lower R_2 values are consistent with an increase in fast (ps–ns) amide bond reorientations, which may reflect an overall increase in the plasticity of the protein. There is an exceptional increase in R_2 for leucine 39, as well as some less pronounced increases, predominantly in the N-terminal domain residues. Interestingly, arginine 37 experiences a significant decrease in R_2, while nearby, leucine 39 is increased. In general, while we observe moderately larger perturbations in the N-terminal domain, the overall dynamics of the protein appear to be increased at higher levels of fluorine labeling.

Estimates of rotational correlation times for the 6, 60 and >95% proteins are shown in Table 2 and were determined from R_2/R_1 values as described previously, with care taken to exclude residues based on evidence of chemical exchange and low NOE values (Kay et al. 1989). Previous studies of calmodulin have established that the two termini effectively reorient independently in solution, with estimates of anisotropic reorientation (10–15%) (Barbato et al. 1992) being much lower than predicted from the barbell-like crystal structure. Thus, we report correlation times for each domain individually, as even at >95% labeling, correlation times plotted per residue suggest two independent correlation times corresponding to residues in the N and C-termini (data not shown). Generally, the global correlation time decreases with increased 3-FPhe enrichment, with a greater difference observed for the N-terminal domain. The higher degree of structural and dynamic perturbations observed for the N-terminal domain is consistent with the effects of fluorine being cumulative, as the N-terminal domain has five phenylalanine residues, while the C-terminal domain has only three.

A decrease in the overall correlation time resulting from >95% 3-FPhe enrichment could result from either increased

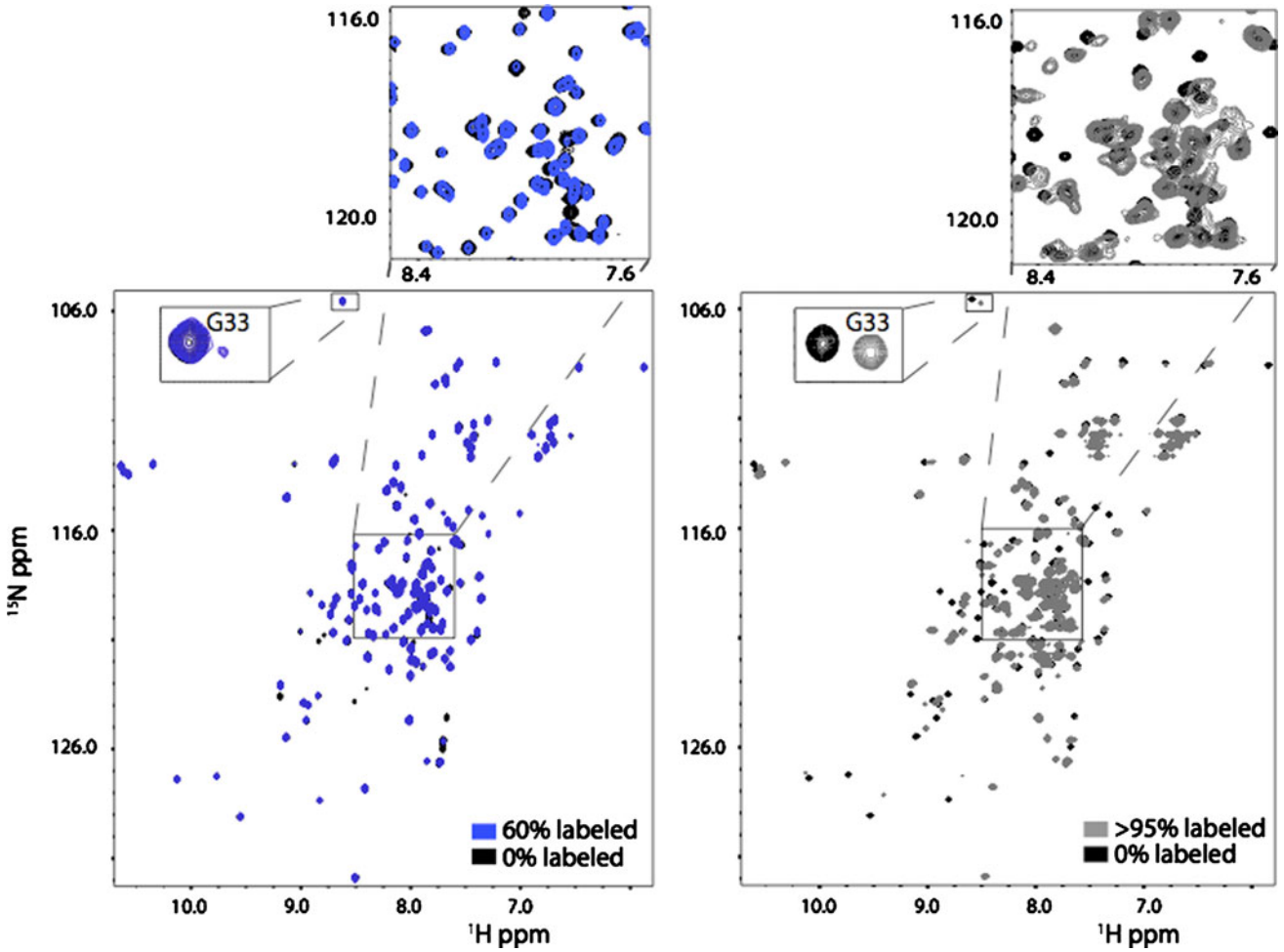

Fig. 2 ^{1}H-^{15}N HSQC spectra of 0% 3-FPhe enriched CaM (*black*) overlaid with analogous spectra of 60% 3-FPhe CaM (*blue*) and >95% 3-FPhe CaM (*grey*). Spectra were collected at 37°C

disorder throughout the protein or a decrease in the hydrodynamic radius of the protein. To confirm that fluorination does not somehow lead to a smaller hydrodynamic radius and thus, faster tumbling, the translational diffusion coefficients of non-fluorinated and >95% ^{19}F-enriched CaM were measured. The diffusion coefficients for 0 and >95% CaM are $1.85 \pm 0.03 \times 10^{-10}$ m^2/s and $1.83 \pm 0.03 \times 10^{-10}$ m^2/s, and relying on the Stokes–Einstein diffusion equation, the corresponding radii of hydration are 17.80 ± 0.08 and 17.95 ± 0.13 Å, respectively. These values are somewhat lower than those obtained previously ($\sim$24 Å) (Weljie et al. 2003), which is likely due to differences in experimental conditions including pH, ionic strength and temperature. The radii of hydration obtained for non—and >95% labeled CaM are identical, within the experimental error, and indicate that the average size of the molecules in solution are the same. Taken together, the ^{1}H-^{15}N HSQC spectra, relaxation rates and translational diffusion data suggest that increased 3-FPhe enrichment results in greater protein flexibility or plasticity, which is manifested as high frequency low amplitude reorientations of the backbone, and an additional slow exchange process between a native and nonnative conformation, involving residues in the N-terminal domain (Jarymowycz and Stone 2006). The presence of multiple minor conformers, observed in the ^{19}F NMR spectra above 80% 3-FPhe enrichment, also supports the notion of slow or intermediate conformational exchange, resulting from the fluorine labels.

Thermal stability of fully and fractionally 3-FPhe labeled CaM

In light of the significant structural and dynamic perturbations observed in CaM with >80% fluorine incorporation, the effect on the overall thermal stability at various labeling levels was assessed using thermal denaturation

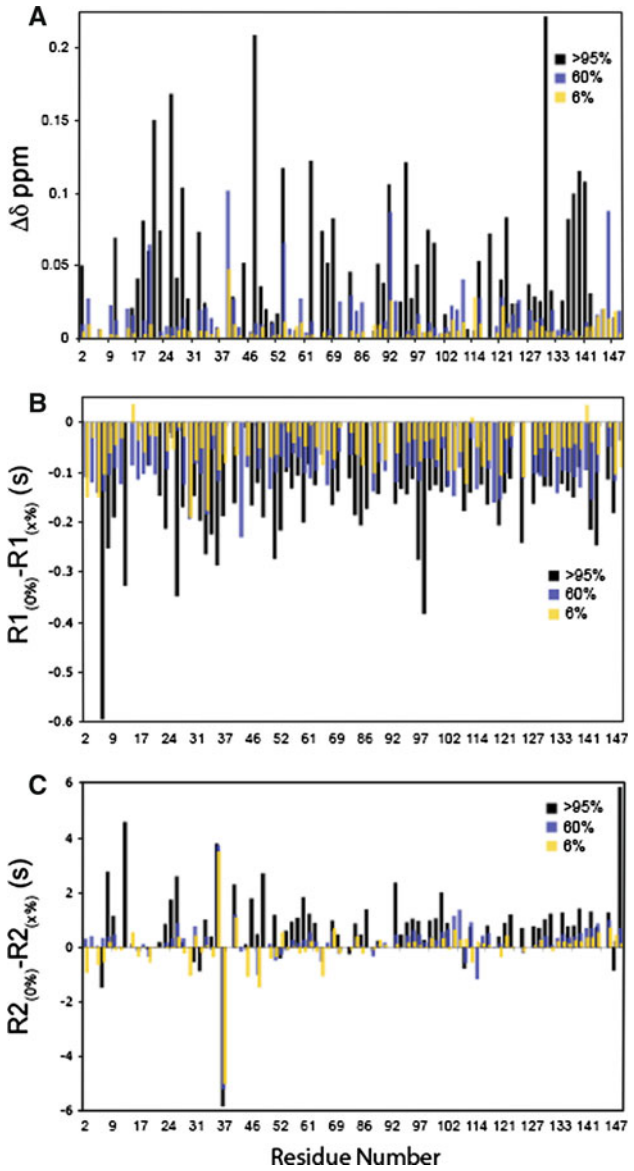

Fig. 3 **a** A histogram of the weighted average of chemical shift perturbations resulting from fluorine incorporation in calmodulin as a function of residue. Shift perturbations were calculated as a weighted average of shifts in both the ^{1}H and ^{15}N dimensions $[\Delta\delta = \sqrt{(\Delta\delta(^{1}\mathrm{H}))^{2} + 0.2(\Delta\delta(^{15}\mathrm{N}))^{2}}]$. Histograms comparing the difference in ^{15}N R_1 (**b**) and ^{15}N R_2 (**c**) values for 0% ^{19}F labeled calmodulin with 6, 60 and >95% ^{19}F labeled calmodulin as a function of residue

monitored by CD spectroscopy. Temperature denaturation experiments were carried out using samples prepared in the calcium-free state due to the very high thermal stability of calcium loaded calmodulin (Masino et al. 2000). The melting temperature of apo-CaM samples with 0, 60, 76, and >95% fluorine incorporation were determined to be 50.8 ± 0.2, 50.5 ± 0.2, 50.0 ± 0.2, 50.7 ± 0.2°C respectively. Although we observe significant changes in our NMR spectra, the overall thermal stability of the proteins are essentially unchanged, within the experimental error.

Table 2 Free energy (ΔG) associated with the conformational exchange between a native and nonnative conformation and overall correlation times (τ_c) for various levels of fluorine enrichment of calmodulin

^{13}F enrichment (%)	ΔG (kJ/mol)	τ_c (ns)	
		N-Terminal domain	C-Terminal domain
0	–	6.4 ± 0.6	7.2 ± 0.6
6	–	8.3 ± 0.5	7.0 ± 0.6
60	13.4	8.0 ± 0.6	6.8 ± 0.6
76	8.1	–	–
>80	0.3	–	–
>95	−4.5	7.1 ± 0.8	6.5 ± 0.5

Conclusions

We demonstrate a fractional fluorine labeling strategy using 3-FPhe CaM which significantly improves ^{19}F and ^{1}H-^{15}N HSQC spectral quality. An optimal balance between NMR signal to noise and spectral quality was found to be at 60–76% enrichment of the fluorinated species. The strategy utilizes biosynthetic protein expression protocols, where the fluorine label is added as a mixture with its native counterpart to affect various levels of fluorine enrichment. Spectral resolution was drastically improved in ^{19}F NMR spectra, where all 8 peaks were resolved in fractionally labeled samples, compared to 6 in fully labeled CaM. In addition, peak line widths were reduced on average by half, and minor conformers previously observed in fully labeled 3-FPhe CaM were absent. ^{1}H-^{15}N HSQC spectra also displayed significantly improved line widths as well as a reduction in chemical shift perturbations. High levels of fluorine incorporation were found to increase the fast timescale dynamics and overall protein disorder as evidenced by ^{15}N relaxation experiments and diffusion measurements. It is somewhat surprising that diffusion measurements, calcium binding experiments and thermal denaturation experiments reveal no discernible difference between the unfluorinated and fully 3-FPhe enriched versions of CaM. Many global properties of the protein appear to remain unchanged upon labeling. In contrast, ^{15}N,^{1}H and in particular, ^{19}F NMR reveal a pronounced effect of fluorination which we attribute to protein plasticity and increased disorder. Generally, fractional ^{19}F-labeling retains native protein structural and dynamic characteristics, while offering the usual advantages of ^{19}F probes in biomolecular NMR.

It is difficult to predict the generality of these results in terms of the benefits of fractional labeling in the case of protein expression with fluoroaromatics. The prevalence of tryptophans in most proteins is on the order of 1.1%, while that of tyrosine and phenylalanine is significantly higher

(on the order of 3.5% where variations of a factor of 2–3 are common in the protein database). In our hands, we have never observed substantial perturbations in ^{1}H-^{15}N HSQCs resulting from 5-fluorotryptophan incorporation, in several proteins, while we have observed substantial perturbations with fluorotyrosine and fluorophenylalanine incorporation. Moreover, since Phe is predominantly situated in the hydrophobic core of soluble proteins, it is more likely that Phe residues may be clustered, and that cumulative effects from fluoro-Phe enrichment would be destabilizing. Even in our study of CaM, we could not identify any ^{19}F-^{19}F NOEs, suggesting that cumulative perturbations were not the result of direct Phe–Phe interactions. Finally, in many studies where single Phe residues were replaced with Tyr (and vice versa) for purposes of assignment, gross perturbations in the ^{19}F NMR spectra were observed. Thus, subtle changes commonly have a profound effect on overall protein structure and stability. Therefore, we cannot for certain argue the generality of our observations except to say that in cases where enrichment of a given fluoroaromatic results in poor NMR spectra or functional assays indicative of reduced stability, fractional enrichment may dramatically improve prospects.

Materials and methods

Protein expression and purification

Preparation of *Xenopus laevis* CaM (residues 1–148) uniformly enriched with ^{15}N and D/L-3-fluorophenylalanine was performed using heterologous expression techniques as previously described (Kitevski-LeBlanc et al. 2009) with modifications at the time of induction to achieve fractional labeling. All chemicals used in protein sample preparation and were obtained from Sigma–Aldrich (Oakville ON, Canada). In general, full (>95%) 3-FPhe labeling is achieved by the addition of 1 g/L of glyphosate with 70 mg/L D/L-tryptophan and 70 mg/L of D/L-tyrosine at an $OD_{600\ nm} = 0.8$. After 1 h, cell cultures typically reach an $OD_{600\ nm} = 1.0$, at which point 35 mg/L of D/L-3-fluorophenylalanine is added followed by agitation and induction of target protein expression using IPTG. Fractional labeling was achieved by adjusting the ratio of D/L-3-fluorophenylalanine to D/L-phenylalanine added prior to induction. For example, 3% 3-FPhe enriched calmodulin requires 25% D/L-3-fluorophenylalanine (i.e. 8.75 mg of D/L-3-fluorophenylalanine and 26.25 mg D/L-phenylalanine). Calmodulin samples corresponding to 6, 60, 76 and >80% incorporation of the fluorinated amino acid required 50% 3-FPhe, 75% 3-FPhe, 85% 3-FPhe, and 98% 3-FPhe enrichment of the total phenylalanine supplied to the media, respectively. The D/L-3-fluorophenylalanine and D/L-phenylalanine mixtures are suspended in a minimal volume of M9 media (but not fully dissolved) immediately prior to addition to shaking cultures. Expression cultures are then agitated until the added amino acids are fully dissolved (<5 min) prior to the addition of IPTG. Samples for NMR were exchanged into 10 mM BIS–TRIS, 0.1 M KCl, 9 mM $CaCl_2$, 0.2% NaN_3 buffer adjusted to pH 8. Samples used for NMR also contained 50 μM D/L-4-fluorophenylalanine as an internal standard for referencing and determination of effective fluorinated protein concentration from ^{19}F NMR experiments.

Fluorine enrichment levels were carefully determined in two steps. First by integration of ^{19}F NMR signal of the 3-FPhe enriched protein, relative to a 50 μM D/L-4-fluorophenylalanine internal standard, we obtain an effective fluorine labeled protein concentration. Then, the total protein concentration in a given NMR sample was determined using the bicinchoninic acid (BCA) protein assay kit (Sigma–Aldrich, Oakville, Ontario, Canada). Enrichment levels were then obtained by taking the ratio of the effective fluorine labeled protein concentration (from integration of ^{19}F NMR) to the total protein concentration (from the BCA protein assay). The estimation of labeling levels using this method is difficult above 76% enrichment due to the effects of inhomogeneous broadening and the presence of minor conformers, which are more difficult to reliably integrate in the ^{19}F NMR spectra. Determination of ^{19}F enrichment in fully labeled CaM samples also suffer from line broadening and multiple conformers. However, such samples are estimated to be at least 95% labeled based on the standard deviation of the noise in the corresponding ^{1}H-^{15}N HSQC spectra, which lack cross-peaks arising from fluorinated phenylalanine residues. Although mass spectrometry has been used successfully in previous studies to obtain quantitative estimates of fluorine enrichment, we were unable to find conditions which provided a CaM sample amenable to quantification of labeling levels using this approach.

NMR experiments

NMR experiments were performed on a 600 MHz Varian Inova spectrometer (Agilent Technologies, Santa Clara, CA) equipped with a 5 mm HCN/FCN triple resonance single gradient salt tolerant cryogenic probe. All NMR samples were approximately 1–1.5 mM in concentration and were maintained at 37°C. ^{1}H-^{15}N HSQC, ^{15}N spin–lattice (T_1) relaxation times, and transverse (T_2) relaxation time were measured using pulse programs obtained from Biopack software (Agilent Technologies, Santa Clara, CA) and were collected in 8 scans with 80 increments spanning 2,000 Hz in the indirect dimension. Typical pulse widths for ^{1}H and ^{15}N were 9.2 and 39.5 μs respectively. ^{15}N spin–lattice (T_1) and transverse (T_2) time constants were

measured using 7 relaxation delays ranging from 0.01 to 0.8 s and 0.01 to 0.13 s respectively. Peak volumes were fit to a single exponential decay function with average standard error of 1.7, 1.5, 1.1 and 2.2% (1.1, 1.1, 1.1, and 1.8%) for T_1 (T_2) data associated with 0, 6, 60 and >95% enrichment respectively. ^{15}N-{^{1}H} steady-state NOEs were measured by collecting spectra in the presence and absence of a 2.5 ms mixing time. NOE values were determined as the ratios of peak intensities measured from spectra with and without proton irradiation and the uncertainty in peak heights were given by the standard deviation of the baseplane noise in the spectra. Uncertainties of the NOE values were obtained by propagating the peak height uncertainty (Nicholson et al. 1992). Diffusion experiments were performed at 37°C using a one-dimensional version of the BPPSTE HSQC as described previously (Rajagopalan et al. 2004). Gradient pulse amplitudes were calibrated from the known diffusion coefficient of HDO at 25°C (Holz and Weingartner 1991). Fifteen gradient amplitude experiments were acquired for each data set with gradient strength varied from 6% to 92% of its maximum power, and all other experimental parameters held constant. Gradient pulses were applied for 2 ms with a recovery time of 0.2 ms, and diffusion delay of 36.8 ms, affording a total signal decay of ~90%. Spectra were processed using VnmrJ and peak heights were obtained with the peak deconvolution program "fitspec". Diffusion coefficients were obtained from the slope of the natural logarithm of normalized peak intensity plotted against the corresponding square of the gradient strengths, and converted to radius of hydration using the Stokes–Einstein equation and the density of pure water (Altieri et al. 1995). ^{19}F NMR experiments were collected using a repetition time of 1.5 s, a spectral width of 8,000 Hz and a typical pulse width of 14 μs. The number of transients used to achieve sufficient signal varied among the fractionally labeled samples, from 30,720 for a 3% 3-FPhe enriched sample, to 1024 for samples with >80% fluorine enrichment. ^{19}F transverse (T_2) relaxation times were measured using a Hahn echo sequence (90°-τ-180°-τ) employing 9 τ values ranging from 0.8 to 11.2 ms. ^{19}F line widths were estimated from ^{19}F NMR spectra where inhomogeneous magnetic field contributions were deemed constant among samples when the line width of the internal standard (D/L-4-fluorophenylalanine) was within 1 Hz between samples. All NMR data was processed using NMRPipe/NMRDraw (Delaglio et al. 1995) and analyzed with NMRView (Johnson and Blevins 1994) unless stated otherwise.

Circular dichroism spectroscopy and thermal denaturation

Thermal stability of 0, 60, 76 and >95% 3-FPhe labeled CaM were measured under calcium free conditions, due to the high thermal stability of calcium saturated calmodulin. Preparation of apo-calmodulin samples was performed as described elsewhere (Kitevski-LeBlanc et al. 2009). Far UV CD spectra were acquired on an Aviv CD spectrometer model 62DS at 25°C. Spectra of 10–20 μM protein, in 0.1 M KCl and 20 mM Tris buffer adjusted to pH 8, were collected from 195 to 260 nm (path length, 0.1 cm; steps, 1 nm; bandwidth, 1 nm; and averaging time 12 s). Thermal denaturation experiments were performed by measuring ellipticity at 222 nm from 15 to 85°C at a rate of 1°C/min. Reversibility of thermal denaturation was assessed to be >90% following cooling to 15°C at a rate of 1°C/min.

Acknowledgments We are grateful to Prof. Mitsu Ikura (University of Toronto) for providing a plasmid for *Xenopous laevis* CaM used in this study and to Prof. Avi Chakrabartty (University of Toronto) for the use of the CD apparatus. We thank Sameer Al-Abdul Wahid (University of Toronto at Mississauga) for assistance with the diffusion experiments. JK-L wishes to acknowledge the Natural Sciences and Engineering Research Council of Canada (NSERC) for a doctoral fellowship. RSP acknowledges NSERC, for financial support through the NSERC discovery grant program (261980) and CIHR for support through a Protein Folding Training Grant.

References

Akcay G, Kumar K (2009) A new paradigm for protein design and biological self-assembly. J Fluor Chem 130:1178–1182

Altieri AS, Hinton DP, Byrd RA (1995) Association of biomolecular systems via pulsed-field gradient Nmr self-diffusion measurements. J Am Chem Soc 117:7566–7567

Anderluh G, Razpotnik A, Podlesek Z, Macek P, Separovic F, Norton RS (2005) Interaction of the eukaryotic pore-forming cytolysin equinatoxin ii with model membranes: F-19 Nmr studies. J Mol Biol 347:27–39

Bann JG, Pinkner J, Hultgren SJ, Frieden C (2002) Real-time and equilibrium F-19-Nmr studies reveal the role of domain-domain interactions in the folding of the chaperone papd. Proc Natl Acad Sci USA 99:709–714

Barbato G, Ikura M, Kay LE, Pastor RW, Bax A (1992) Backbone dynamics of calmodulin studied by N-15 relaxation using inverse detected 2-dimensional Nmr-spectroscopy-the central Helix is flexible. Biochemistry 31:5269–5278

Bilgiçer B, Fichera A, Kumar K (2001) A coiled coil with a fluorous core. J Am Chem Soc 123:4393–4399

Broos J, Maddalena F, Hesp BH (2004) In vivo synthesized proteins with monoexponential fluorescence decay kinetics. J Am Chem Soc 126:22–23

Campos-Olivas R, Aziz R, Helms GL, Evans JNS, Gronenborn AM (2002) Placement of F-19 into the center of Gb1: effects on structure and stability. FEBS Lett 517:55–60

Crivici A, Ikura M (1995) Molecular and structural basis of target recognition by calmodulin. Annu Rev Biophys Biomol Struct 24:85–116

Danielson MA, Falke JJ (1996) Use of F-19 Nmr to probe protein structure and conformational changes. Annu Rev Biophys Biomol Struct 25:163–195

Delaglio F, Grzesiek S, Vuister GW, Zhu G, Pfeifer J, Bax A (1995) Nmrpipe-a multidimensional spectral processing system based on unix pipes. J Biomol NMR 6:277–293

Duewel H, Daub E, Robinson V, Honek J (2001) Elucidation of solvent exposure, side-chain reactivity, and steric demands of the trifluoromethionine residue in a recombinant protein. Biochemistry 40:13167–13176

Geddes CD (2009) Reviews in Fluorescence 2008, vol 5, illustrated ed. Springer

Hoeflich KP, Ikura M (2002) Calmodulin in action: diversity in target recognition and activation mechanisms. Cell 108:739–742

Holz M, Weingartner H (1991) Calibration in accurate spin-echo self-diffusion measurements using H-1 and less-common nuclei. J Magn Reson 92:115–125

Jarymowycz VA, Stone MJ (2006) Fast time scale dynamics of protein backbones: Nmr relaxation methods, applications, and functional consequences. Chem Rev 106:1624–1671

Johnson BA, Blevins RA (1994) Nmr view-a computer-program for the visualization and analysis of Nmr data. J Biomol NMR 4:603–614

Kay LE, Torchia DA, Bax A (1989) Backbone dynamics of proteins as studied by N-15 inverse detected heteronuclear Nmr-spectroscopy-application to staphylococcal nuclease. Biochemistry 28:8972–8979

Kitevski-LeBlanc JL, Evanics F, Prosser RS (2009) Approaches for the measurement of solvent exposure in proteins by F-19 Nmr. J Biomol NMR 45:255–264

Kitevski-Leblanc JL, Evanics F, Scott Prosser R (2010) Approaches to the assignment of (19)F resonances from 3-fluorophenylalanine labeled calmodulin using solution state NMR. J Biomol NMR 47:113–123

Li HL, Frieden C (2007) Observation of sequential steps in the folding of intestinal fatty acid binding protein using a slow folding mutant and F-19 Nmr. Proc Natl Acad Sci USA 104:11993–11998

Luck LA, Falke JJ (1991) F-19 Nmr-studies of the D-galactose chemosensory receptor.1. Sugar binding yields a global structural-change. Biochemistry 30:4248–4256

Masino L, Martin SR, Bayley PM (2000) Ligand binding and thermodynamic stability of a multidomain protein, calmodulin. Protein Sci 9:1519–1529

Nicholson LK, Kay LE, Baldisseri DM, Arango J, Young PE, Bax A, Torchia DA (1992) Dynamics of methyl-groups in proteins as studied by proton-detected C-13 Nmr-spectroscopy-application to the leucine residues of staphylococcal nuclease. Biochemistry 31:5253–5263

Okano H, Cyert MS, Ohya Y (1998) Importance of phenylalanine residues of yeast calmodulin for target binding and activations. J Biol Chem 273:26375–26382

Quint P, Ayala I, Busby SA, Chalmers MJ, Griffin PR, Rocca J, Nick HS, Silverman DN (2006) Structural mobility in human manganese superoxide dismutase. Biochemistry 45:8209–8215

Rajagopalan S, Chow C, Raghunathan V, Fry C, Cavagnero S (2004) Nmr spectroscopic filtration of polypeptides and proteins in complex mixtures. J Biomol NMR 29:505–516

Rozovsky S, Jogl G, Tong L, McDermott AE (2001) Solution-state Nmr investigations of triosephosphate isomerase active site loop motion: ligand release in relation to active site loop dynamics. J Mol Biol 310:271–280

Schuler B, Kremer W, Kalbitzer HR, Jaenicke R (2002) Role of entropy in protein thermostability: folding kinetics of a hyperthermophilic cold shock protein at high temperatures using F-19 Nmr. Biochemistry 41:11670–11680

Tang Y, Ghirlanda G, Petka W, Nakajima T, DeGrado W, Tirrell D (2001) Fluorinated Coiled-coil proteins prepared in vivo display enhanced thermal and chemical stability. Angew Chem Int Ed 40:1494–1496

Visser NV, Westphal AH, Nabuurs SM, van Hoek A, van Mierlo CPM, Visser A, Broos J, van Amerongen H (2009) 5-Fluorotryptophan as dual probe for ground-state heterogeneity and excited-state dynamics in apoflavodoxin. FEBS Lett 583:2785–2788

Weljie A, Yamniuk A, Yoshino H, Izumi Y, Vogel H (2003) Protein conformational changes studied by diffusion Nmr spectroscopy: application to helix-loop-helix calcium binding proteins. Protein Sci 12:228–236

Woll MG, Hadley EB, Mecozzi S, Gellman SH (2006) Stabilizing and destabilizing effects of phenylalanine ->F-5-phenylalanine mutations on the folding of a small protein. J Am Chem Soc 128:15932–15933

Woolfson DN (2001) Core-directed protein design. Curr Opin Struct Biol 11:464–471

Xiao GY, Parsons JF, Tesh K, Armstrong RN, Gilliland GL (1998) Conformational changes in the crystal structure of rat glutathione transferase M1–1 with global substitution of 3-fluorotyrosine for tyrosine. J Mol Biol 281:323–339